Disposition Studies in Rats. a. Animals. Thirty-six male (group I) and 36 female (group II) Charles River Sprague–Dawley rats (100–150 g) were used. During a 1–2-week acclimation period, the rats were maintained on standard ration (Wayne Lab Blox) and had free access to water. The rats were fasted for 18 h prior to drug treatment. Three rats from both groups I and II were housed in individual glass metabolism cages that separated urine and feces. The remaining rats from each group were divided into 11 subgroups of three animals, and each subgroup was housed in a separate cage. The cages and animals were marked as to the time of sacrifice. The cages were set up so that the rats could not come into contact with excreta.

b. Drug Treatment and Sample Collection. The rats were weighed just prior to treatment and received an appropriate dose (~0.5 mL) orally of 10 mg/kg of 2-^{14}C-**2** dissolved in 0.02 N lactic acid (0.055 mCi/animal). The subgroups (three animals each) were killed at 0.25, 0.5, 0.75, 1.0, 1.5, 2, 3, 4, 6, 10, and 24 h after treatment. Rats from each group housed in metabolism cages were killed at 72 h after the dose. Blood (3–5 mL) was obtained from each rat; it was allowed to clot at room temperature for about 30 min and centrifuged to remove serum. Serum was stored frozen (−20 °C) until assay. From each of the rats, the following tissues were obtained: liver, kidney, muscle, brain, lung, stomach, intestines, and testes or ovaries. Cumulative urine and feces were collected at 24-h intervals for the rats housed in metabolism cages.

c. Assay Methods. Samples were analyzed for total radiocarbon by combustion and LSC. Two-dimensional TLC autoradiography was used to define the pattern of urinary metabolites, including the extent of conjugation (analysis of urine before and after treatment with β-glucuronidase and sulfatase). Quantities of intact drug and the major metabolite in blood and excreta were measured by LSC following TLC separation.

Isolation and Identification of a Metabolite of 2. To obtain a sufficient quantity of the **2** metabolite for characterization, 10 rats were dosed on 2 consecutive days with unlabeled **2** (20 mg/kg), and urine was collected for 48 h. To expedite purification of the metabolite, some of the urine from rats that received radiolabeled drug was added to the urine from the cold experiment. The combined urine was applied to an XAD-2 column, which was washed with water and eluted with methanol. The methanol fraction had 91% of the radioactivity. After evaporation of the solvent, the residue was applied to several 0.5-mm, 20 × 20 silica gel TLC plates, which were developed with a 20% aqueous *n*-PrOH solvent system. The major metabolite ($R_f \cong 0.6$) was eluted from the silica gel with MeOH and further purified by HPLC with a μ-Bondapak C_{18} column with an acetonitrile/water (1:4) mobile phase. The solvent was evaporated, and the residue analyzed by MS. The accurate mass of the highest ion observed was determined by peak matching at 10 000 resolution, 10% valley definition, and found to be 312.1581 (calcd for $C_{17}H_{20}N_4O_2$ 312.1576). The NMR spectrum indicated that one isopropyl methyl was altered: NMR (Me_2SO-d_6) δ 1.11 (m, 6), 1.25 (d, 3), 3.1–3.6 (m, 2), 3.42 (s, 2), 5.59 (s, 2), 5.92 (s, 2), 6.57 (d, 1), 6.75 (d, 1), 7.40 (s, 1). These spectral data were consistent with a **2,4-diamino-5-[4-hydroxy-3-isopropyl-5-(α-carboxyethyl)benzyl]pyrimidine** structure (**43**) for the metabolite.

Registry No. **2**, 42310-33-8; 2-^{14}C-**2**, 110798-52-2; **3**, 4433-40-3; **4**, 128-39-2; **5**, 66-22-8; **6**, 88-27-7; **7**, 73943-43-8; **8**, 84876-25-5; **9**, 73943-44-9; **10**, 110798-40-8; **11**, 73554-80-0; **12**, 42310-45-2; **13**·HCl, 110798-41-9; **14** (isomer 1), 110798-42-0; **14** (isomer 2), 110798-48-6; **15** (isomer 1), 110798-43-1; **15** (isomer 2), 110798-49-7; **16**, 110798-44-2; **16**·HCl, 110798-50-0; **17**, 2078-54-8; **18**, 10537-86-7; **19**, 110798-45-3; **20**, 108402-07-9; **21**, 4542-47-6; **22**, 110798-46-4; **23**, 110798-47-5; 2-^{14}C-**23**, 110798-51-1; **24**, 42310-36-1; **25**, 105639-88-1; **26**, 36821-97-3; **27**, 73554-79-7; **28**, 73554-78-6; **29**, 105639-89-2; **30**, 73576-30-4; **31**, 105639-85-8; **32**, 36821-88-2; **33**, 105639-86-9; **34**, 36821-94-0; **35**, 36821-90-6; **36**, 105639-87-0; **37**, 39667-06-6; **38**, 110798-54-4; **39**, 110798-55-5; **40**, 110798-56-6; **41**, 110798-57-7; **62**, 110798-53-3; 2-[^{14}C]guanidine hydrochloride, 73549-39-0; benzyl bromide, 100-39-0; guanidine hydrochloride, 50-01-1.

(18) Gibaldi, M.; Perrier, D. in *Pharmacokinetics, Drugs, and the Pharmaceutical Sciences I*; Marcel Dekker: New York, 1975; pp 293–296.

Evaluation of the Importance of Hydrophobic Interactions in Drug Binding to Dihydrofolate Reductase

Kazunari Taira and Stephen J. Benkovic*

Department of Chemistry, 152 Davey Laboratory, The Pennsylvania State University, University Park, Pennsylvania 16802, and Fermentation Research Institute, Agency of Industrial Science and Technology, MITI, Tsukuba Science City, Ibaraki 305, Japan. *Received June 22, 1987*

The interaction of dihydrofolate reductase (DHFR) from *Escherichia coli* with drugs such as methotrexate (MTX) and 2,4-diamino-6,7-dimethylpteridine (DAM) has been studied by means of site-directed mutagenesis, fluorescence spectroscopy, and steady-state as well as transient kinetics. A strictly conserved residue at the dihydrofolate binding site of DHFR, phenylalanine-31, has been replaced with tyrosine or valine to ascertain the importance for binding of this hydrophobic amino acid, which interacts with both the pteridine ring and the *p*-aminobenzoyl moiety. The first mutation (Phe-31 → Tyr) has a minimal effect on the binding of the classical inhibitor, DAM. On the other hand, the second mutation (Phe-31 → Val) has increased the dissociation constant of DAM from the DHFR·NADPH·DAM ternary complex over 150-fold (>3 kcal/mol). The dissociation constant of DAM from the (Val31-DHFR)·DAM binary complex was too large to be measured fluorometrically. More importantly, these mutations have decreased the overall tight binding of MTX, from 100- to 140-fold (corresponding to a loss of binding energy of 2.2–2.4 kcal/mol) for the Tyr-31 and Val-31 mutants, respectively. These results indicate that hydrophobic interactions between MTX and DHFR are at least as important as formation of the MTX·DHFR salt bridge in the tight binding of MTX.

Dihydrofolate reductase (5,6,7,8-tetrahydrofolate: $NADP^+$ oxidoreductase, EC 1.5.1.3; DHFR) catalyzes the NADPH-dependent reduction of 7,8-dihydrofolate (H_2F) to 5,6,7,8-tetrahydrofolate (H_4F). The enzyme is necessary for maintaining intracellular pools of H_4F and its derivatives which are essential cofactors in the many important biosynthetic reactions which require the transfer of one-carbon units. An anti-folate drug, methotrexate (MTX), differs from the natural folates in only two positions: a methyl group replaces the N-10 hydrogen and an amino group replaces the C-4 keto function of the pteridine ring. These slight molecular changes produce a potent inhibition of DHFR and ultimately inhibit the synthesis of purines, pyrimidines, and DNA due to the loss of nucleotide production. Because of this enzyme's biological and pharmacological importance, it has been the subject of extensive studies, both structural and kinetic, over the past three decades.[1-3]

0022-2623/88/1831-0129$01.50/0

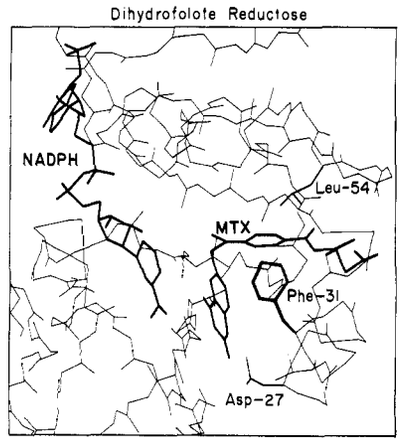

Figure 1. The active site of DHFR showing the interaction of Phe-31 with both the pteridine ring and the *p*-aminobenzoyl moiety of MTX.

An aspect of major interest regarding 2,4-diamino heterocyclic inhibitors of DHFR like MTX has been the molecular basis for their tight binding. In recent years a substantial body of structural information on this enzyme and its anti-folate complexes has become available from X-ray crystallography[4-6] and NMR spectroscopy[7,8] (Figure 1). In particular, the existence of a salt bridge in the DHFR·MTX complex between an active site Asp-27 and the 4-amino group of the MTX which was inferred from X-ray crystallography has been confirmed by UV[9,10] and NMR spectroscopy.[11-13] The very strong interaction of the protonated heterocyclic ring of the inhibitor and the Asp-27 of the enzyme side chain is evidenced by the pK_a of the bound MTX that is >10 even though the pK_a of the unbound MTX is ca. 5.3. Ab initio molecular orbital calculations on neutral and protonated 2,4-diamino-6-methylpteridine led to the conclusion that the salt bridge between N-1 and the Asp-27 is the most important component of the binding of protonated MTX.[14]

Site-directed mutagenesis has become a powerful tool for elucidation of the functional role of individual amino acids in a protein.[15-33] A number of active site specific

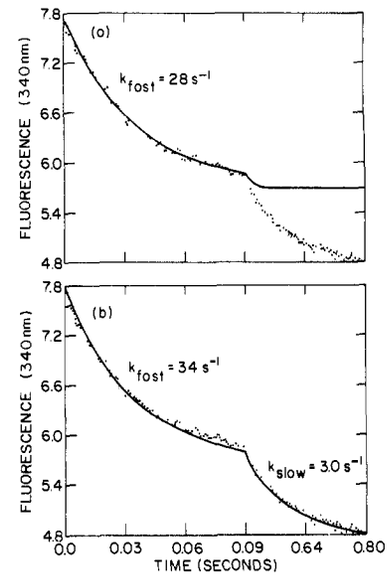

Figure 2. Time course of the enzyme fluorescence decay upon mixing of 0.28 μM Tyr31-DHFR with 2.0 μM methotrexate (MTX) at 25 °C and pH 6.0 in MTEN buffer. Data were collected into 250 memory points, with the initial 150 points employed for the period of 0–0.09 s and the following 100 points for the period of 0.09–0.80 s. The data was fit to (a) a single-exponential model employing the initial 150 data points or (b) a double-exponential model utilizing the entire 250 data points. A single-exponential model could not be used for fitting the entire 250 points.

Scheme I

$$E_1 + L_1 \underset{k_{off}}{\overset{k_{on}}{\rightleftharpoons}} E_1{\cdot}L_1 + L_2 \underset{k'_{off}}{\overset{k'_{on}}{\rightleftharpoons}} E_1{\cdot}L_1{\cdot}L_2$$
$$k_1 \downarrow\uparrow k_2$$
$$E_2$$

mutants have been constructed, and in some cases, crystallographic as well as solution studies of the mutants are

(1) Blakley, R. L. In *Folates and Pterins*, Blakley, R. L., Benkovic, S. J., Eds.; Wiley: New York, 1985; p 191–253.
(2) Blaney, J. M.; Hansch, C.; Silipo, C.; Vittoria, A. *Chem. Rev.* **1984**, *84*, 333–407.
(3) Gready, J. E. *Adv. Pharmacol. Chemother.* **1980**, *17*, 37–102.
(4) Bolin, J. T.; Filman, D. J.; Matthews, D. A.; Hamlin, R. C.; Kraut, J. *J. Biol. Chem.* **1982**, *257*, 13 650–13 662.
(5) Filman, D. J.; Bolin, J. T.; Matthews, D. A.; Kraut, J. *J. Biol. Chem.* **1982**, *257*, 13 663–13 672.
(6) Matthews, D. A.; Bolin, T. J.; Burridge, J. M.; Filman, D. J.; Volz, K. W.; Kaufman, B. T.; Beddell, C. R.; Champness, J. N.; Stammers, D. K.; Kraut, J. *J. Biol. Chem.* **1985**, *260*, 381–391.
(7) Hammond, S. J.; Birdsall, B.; Searle, M. S.; Roberts, G. C. K.; Feeney, J. *J. Mol. Biol.* **1986**, *188*, 81–97.
(8) Searle, M. S.; Hammond, S. J.; Birdsall, B.; Roberts, G. C. K.; Feeney, J.; King, R. W.; Griffiths, D. V. *FEBS Lett.* **1986**, *194*, 165–170.
(9) Hood, K.; Roberts, G. C. K. *Biochem. J.* **1978**, *171*, 357–366.
(10) Stone, S. R.; Morrison, J. F. *Biochemistry* **1984**, *23*, 2753–2758.
(11) Cocco, L.; Temple, C., Jr.; Montgomery, J. A.; London, R. E.; Blakley, R. L. *Biochem. Biophys. Res. Commun.* **1981**, *100*, 413–419.
(12) Cocco, L.; Groff, J. P.; Temple, C., Jr.; Montgomery, J. A.; London, R. E.; Blakley, R. L. *Biochemistry* **1981**, *20*, 3972–3978.
(13) London, R. E.; Howell, E. E.; Warren, M. S.; Kraut, J.; Blakley, R. L. *Biochemistry* **1986**, *25*, 7235–7243.
(14) Schlegel, H. B.; Poe, M.; Hoogsteen, K. *Mol. Pharmacol.* **1981**, *20*, 154–158.
(15) Beck von Bodman, S.; Schuler, M. A.; Jollie, D. R.; Sligar, S. G. *Proc. Natl. Acad. Sci. U.S.A.* **1986**, *83*, 9443–9447.
(16) Chen, J.-T.; Mayer, R. J.; Fierke, C. A.; Benkovic, S. J. *J. Cell. Biochem.* **1985**, *29*, 73–82.
(17) Chen, J.-T.; Taira, K.; Tu, C.-P. D.; Benkovic, S. J. *Biochemistry* **1987**, *26*, 4093–4100.
(18) Clarke, A. R.; Wigley, D. B.; Chia, W. N.; Barstow, D.; Atkinson, T.; Holbrook, J. J. *Nature (London)* **1986**, *324*, 699–702.
(19) Craik, C. S.; Largman, C.; Fletcher, T.; Roczniak, S.; Barr, P. J.; Fletterick, R.; Rutter, W. *J. Science (Washington, D.C.)* **1985**, *228*, 291–297.
(20) Dalbadie-McFarland, G.; Cohen, L. W.; Riggs, A. D.; Morin, C.; Itakura, K.; Richards, J. H. *Proc. Natl. Acad. Sci. U.S.A.* **1982**, *79*, 6409–6413.
(21) Dalbadie-McFarland, G.; Neitzel, J. J.; Richards, J. H. *Biochemistry* **1986**, *25*, 332–338.
(22) Estell, D. A.; Graycar, T. P.; Wells, J. A. *J. Biol. Chem.* **1985**, *260*, 6518–6521.
(23) Estell, D. A.; Graycar, T. P.; Miller, J. V.; Powers, D. B.; Burnier, J. P.; Ng, P. G.; Wells, J. A. *Science (Washington, D.C.)* **1986**, *233*, 659–663.
(24) Fersht, A. R.; Shi, J.-P.; Wilkinson, A. J.; Blow, D. M.; Carter, P.; Waye, M. M. Y.; Winter, G. P. *Angew. Chem., Int. Ed. Engl.* **1984**, *23*, 467.
(25) Ghosh, S. S.; Bock, S. C.; Rokita, S. E.; Kaiser, E. T. *Science (Washington, D.C.)* **1986**, *231*, 145–148.
(26) Howell, E. E.; Villafranca, J. E.; Warren, M. S.; Oakley, S. J.; Kraut, J. *Science (Washington, D.C.)* **1986**, *231*, 1123–1128.
(27) Itakura, K.; Rossi, J. J.; Wallace, R. B. *Annu. Rev. Biochem.* **1984**, *53*, 323–356.
(28) Leatherbarrow, R. J.; Fersht, A. R. *Protein Engineering* **1986**, *1*, 7–16.
(29) Taira, K.; Chen, J.-T.; Mayer, R. J.; Benkovic, S. J. *Bull. Chem. Soc. Jpn.* **1987**, *60*, 3017–3024.
(30) Taira, K.; Chen, J.-T.; Fierke, C. A.; Benkovic, S. J. *Bull. Chem. Soc. Jpn.* **1987**, *60*, 3025–3030.

available.[26] Conversion of Asp-27 to Asn or Ser generates two new enzyme forms in which the binding affinity for MTX (K_D, pH 7.0, 4 °C) is reduced from 0.07 nM (wild type) to 1.9 nM and 210 nM for the Asn-27 and Ser-27 enzymes, respectively. X-ray structural results on both mutant E·MTX complexes revealed that neither the MTX binding geometry nor the detailed three-dimensional topography of the dihydrofolate reductase was altered by the mutation. NMR spectroscopy of bound MTX to these mutants provided direct evidence for the absence of a salt bridge.[13] These results enabled one to estimate the binding energy due to the salt bridge: K_D(Asn-27)/K_D(Asp-27) ≈ 27 (1.8 kcal/mol). This 1.8 kcal/mol loss in binding energy upon Asp-27 → Asn mutation, however, is insufficient to explain the ca. 10^4-fold difference in binding between substrate and inhibitor.

We have thus used site-directed mutagenesis to examine the role of Phe-31, which exhibits van der Waals interactions with both the pteridine ring and the *p*-aminobenzoyl moiety, in catalysis[17,29,30] as well as drug binding.[31] In the following study we describe for MTX and 2,4-diamino-6,7-dimethylpteridine (DAM) the measurement of the thermodynamic dissociation constants and individual rate constants for their binding to the wild-type (Phe-31) and two mutant (Tyr-31 and Val-31) *E. coli* dihydrofolate reductases. The resultant free energy diagrams for complex formation were used to determine the specific effects of the mutation on drug binding and to evaluate quantitatively hydrophobic interactions.

Results

Binding of Inhibitors to DHFR. The rate of binding of ligands to DHFR in either the cofactor or the folate binding sites can be measured by following the quenching of the intrinsic enzyme fluorescence at 340 nm as a function of time after mixing of the enzyme with a ligand in a stopped-flow apparatus.[34-39] In the formation of binary complexes of DHFR at saturating substrate concentration, two exponentials of similar amplitude were observed: a rapid ligand-dependent phase followed by a slow ligand-independent phase. In the formation of ternary from binary complexes, a single ligand-dependent exponential was observed as previously described by Dunn, Cayley, Batchelor, and King.[34-36] They concluded that this behavior was due to the mechanism shown in Scheme I where substrate binds rapidly to only one (E_1) of two enzyme conformers (E_1 and E_2) and the interconversion rate between conformers is slow ($k_2 \approx 0.03$ s^{-1}).

In contrast, inhibitors such as methotrexate (MTX) and trimethoprim (TMP) caused only a rapid quenching of the fluorescence, however, the latter decay did not follow a single exponential but was fit with precision to two exponentials.[36] Since both phases were dependent on the

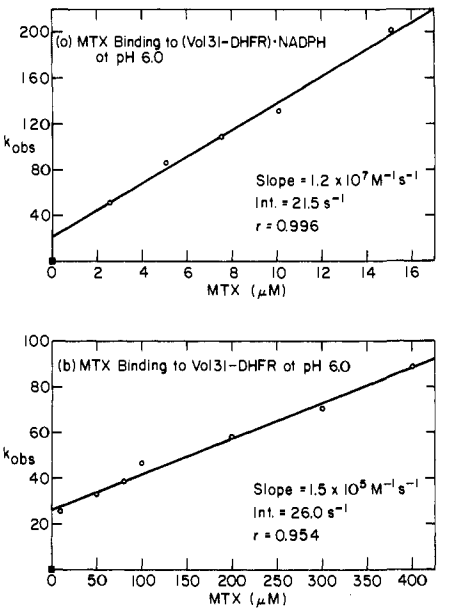

Figure 3. Dependence of observed pseudo-first-order rate constants on MTX concentration. (a) (Val31-DHFR)·NADPH binary complex was mixed with MTX. (b) Val31-DHFR apoenzyme was mixed with MTX at 25 °C and pH 6.0 in MTEN buffer.

Scheme II

$$E{\cdot}L_1 \underset{k_{fwd}}{\overset{k_{rev}}{\rightleftharpoons}} E + L_1$$

$$E + L_2 \underset{k_{diss}}{\overset{k_{trap}}{\rightleftharpoons}} E{\cdot}L_2$$

MTX concentration, both forms of the enzyme, E_1 and E_2, are capable of binding MTX rapidly so that complex formation is complete before isomerization ($K_{eq} = k_1/k_2$) is possible.

Shown in Figure 2a and 2b is the time-dependent quenching of the fluorescence of the Tyr-31 mutant DHFR upon MTX binding. The character of the decay curve is identical with that of the wild-type enzyme except for the specific rate constants. The entire decay curve over 0.8 s at a final MTX concentration of 1.0 μM could not be described by a single exponential (significant deviation especially in the fast phase) but could be described by two exponentials as shown in Figure 2b. Upon a closer examination of Figure 2b, simulation of the fast phase by two exponentials show a small systematic deviation, which is not readily noticeable unless data are collected by utilizing two time scales as in Figure 2 (150 points have been used for the initial 0.09 s and the remaining 100 points for up to 0.8 s). The initial decay could be described more accurately if three to four half-lives of the fast phase were fit to a single exponential (Figure 2a) neglecting the slow phase. Consequently, in this study our analysis will focus on the fast phase of MTX binding, since MTX associates primarily with a preferred conformer in a process that has a direct dependence on the ligand concentration.

The observed first-order rate constants for the fast phase increase linearly with the ligand concentration, showing no sign of saturation as shown in Figure 3a and 3b for the MTX binding to the (Val31-DHFR)·NADPH binary holoenzyme complex and Val31-DHFR apoenzyme, respectively. For a simple association reaction, the observed rate constant under pseudo-first-order conditions may be approximated by

$$k_{obsd} = k_{on}[L] + k_{off} \quad (1)$$

where k_{on} and k_{off} are the association and dissociation rate

(31) Taira, K.; Fierke, C. A.; Chen, J.-T.; Johnson, K. A.; Benkovic, S. J. *Trends Biochem. Sci. (Pers. Ed.)* **1987**, *12*, 275–278.
(32) Tsuji, F. I.; Inoue, S.; Goto, T.; Sakaki, Y. *Proc. Natl. Acad. Sci. U.S.A.* **1986**, *83*, 8107–8111.
(33) Villafranca, J. E.; Howell, E. E.; Voet, D. H.; Strobel, M. S.; Ogden, R. C.; Abelson, J. N.; Kraut, J. *Science (Washington, D.C.)* **1983**, *222*, 782–788.
(34) Dunn, S. M. J.; King, R. W. *Biochemistry* **1980**, *19*, 766–773.
(35) Dunn, S. M. J.; Batchelor, J. G.; King, R. W. *Biochemistry* **1978**, *17*, 2356–2364.
(36) Cayley, P. J.; Dunn, S. M. J.; King, R. W. *Biochemistry* **1981**, *20*, 874–879.
(37) Blakley, R. L.; Cocco, L. *Biochemistry* **1985**, *24*, 4704–4709.
(38) Blakley, R. L.; Cocco, L. *Biochemistry* **1985**, *24*, 4772–4777.
(39) Fierke, C. A.; Johnson, K. A.; Benkovic, S. J. *Biochemistry* **1987**, *26*, 4085–4092.

Table I. Rate Constants for the Initial Complex (EH·L) Formation and Dissociation Rate Constants from the Final Complexes at pH 6.0[a]

inhibitor	DHFR	k_{on},[b] M^{-1} s^{-1}	k_{off},[b] s^{-1}	k_r,[c] s^{-1}
MTX	Wt. (Phe-31)[d]	$(3.6 \pm 0.2) \times 10^7$[e]	12 ± 2[e]	0.0051 ± 0.0005
	Tyr-31[f]	$(1.1 \pm 0.2) \times 10^7$	26 ± 5	0.20 ± 0.02
	Val-31	$(1.5 \pm 0.3) \times 10^5$	26 ± 10	0.048 ± 0.001
DAM	Phe-31	$(1.2 \pm 0.1) \times 10^7$	35 ± 5	24 ± 1
	Tyr-31	$(6.8 \pm 0.5) \times 10^6$	25 ± 2	25 ± 2
	Val-31[g]	–	–	–

[a] The enzymes were excited at 290 nm, and the fluorescence change was monitored at 340 nm at 25 °C. The buffer used was MTEN buffer. [b] Determined from linear plots of k_{obsd} vs inhibitor concentration, such as shown in Figure 3. The slope and the intercept represent k_{on} and k_{off}, respectively. [c] Determined by competition experiments. DHFR (0.5–1.0 μM) was preincubated with either MTX (2.0 μM) or DAM (10 μM) and then trapped with TMP (1000 μM) for the DHFR·MTX complexes and with MTX (100–200 μM) for the DHFR·DAM complexes. [d] At pH 9.0, k_{on} and k_{off} are $(3.5 \pm 0.3) \times 10^7$ M^{-1} s^{-1} and 10 ± 2 s^{-1}, respectively. [e] Fierke and Benkovic, personal communication. [f] At pH 9.0, k_{on} and k_{off} are $(0.99 \pm 0.2) \times 10^7$ M^{-1} s^{-1} and 32 ± 3 s^{-1}, respectively. [g] Unable to be measured.

constants, respectively. Thus, in a linear plot of k_{obsd} versus [L] as in Figure 3, the slope is k_{on} and the intercept is k_{off}. It is noteworthy that the association rate constant of MTX for the holoenzyme (Figure 3a) is about 2 orders of magnitude faster than the on rate constant for the apoenzyme (Figure 3b), although the off rate constants (the intercepts) are nearly identical. The rate constants for the binding of MTX and DAM to the three forms of DHFR employed are summarized in Table I.

Measurements of Dissociation Rate Constants by Competition Experiments. The dissociation rate constant of a ligand from the DHFR–ligand complex ($E{\cdot}L_1$) can be measured through trapping by a second ligand (L_2), which competes for the same binding site[36,40] (Scheme II). In this technique, the first enzyme–ligand complex ($E{\cdot}L_1$) is mixed with a large excess of a second ligand (L_2), which competes for the binding site, and the formation of the new enzyme–ligand complex ($E{\cdot}L_2$) is monitored by a fluorescence change due to the difference in fluorescence quenching for the two ligands. When $k_{rev} \ll k_{trap}[L_2] \gg k_{fwd}[L_1]$, the fluorescence change is attributable to the conversion of $E{\cdot}L_1$ to $E{\cdot}L_2$ characterized by a single exponential with the dissociation rate constant (k_{rev}) for L_1. The validity of these conditions is checked by showing that k_{obsd} for this reaction, which ought to be equal to k_{rev}, is independent of the concentration of the trapping ligand, L_2.

As shown in Figure 4, for the measurement of the dissociation of MTX from the (Tyr31-DHFR)·MTX binary complex by trapping the latter with trimethoprim (TMP), the observed increase in fluorescence with time was described well by a single exponential. This, together with the fact that the observed rate constant ($k_{obsd} = k_r$) was independent of the concentration of TMP, indicated that the above trapping conditions were satisfied. The increase in fluoresence upon replacement of MTX by TMP is expected, since TMP is known to quench the enzyme fluorescence less efficiently.[36] However, the similar replacement of MTX by TMP within the DHFR·NADPH·MTX ternary complex by TMP results in a decrease in the fluorescence of the ternary complex, although

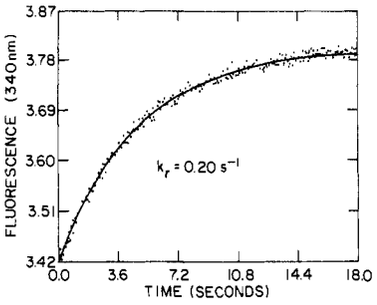

Figure 4. Time course of the fluorescence changes upon mixing of 1 mM trimethoprim (TMP) with a solution containing 1 μM Tyr31-DHFR and 2 μM MTX at 25 °C and pH 6.0 in MTEN buffer. The curve is the best-fit single exponential. The data is fit to about five half-lives.

Scheme III

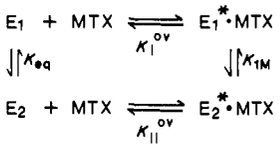

the signal is very weak (data not shown). This difference may originate from the differential synergistic effects of NADPH toward various ligands. In fact NADPH exhibits much higher synergism toward TMP than MTX.[41]

Dissociation rate constants (k_r) determined with this technique for MTX and DAM in MTEN buffer at 25 °C are given in the last column of Table I. For these measurements, five half-lives of data were collected and fit to a single exponential.

Measurements of Thermodynamic Dissociation Constants. The binding of MTX or DAM to free DHFR was determined by following the decrease in enzyme fluorescence that occurs on the formation of DHFR–ligand complexes. The data for the resulting fluorescence titration curves were fit to eq 8 in order to calculate the thermodynamic dissociation constants (K_D). Values for K_D's are listed in Table II. Since MTX binds to both the E_1 and E_2 forms of the enzyme, the overall dissociation constant is potentially reflective of several equilibria (Scheme III). However, since $K_{eq} < 1$ (Table III)[34-36] and structural studies are consistent with a single binary complex ($K_{1M} \approx K_{ii}^{ov}K_{eq}/K_i^{ov} > 1$), the overall dissociation constant is a satisfactory measure of the equilibrium between E_1 and E_2 and E_1*·MTX (the ultimate binary complex). In accord with the finding of Cayley et al.[36] that the K_D's for NADPH and folate are pH-independent for the wild-type enzyme over the pH range of 5–7.5, the same K_D's including those for the mutants are also pH-independent over a pH range of 7–8.5. In contrast, the K_D's for MTX are clearly pH-dependent[42] and correlate well with pK_a of 6.5[39] and 5.9[30] for the wild type and two mutant enzymes respectively (data not shown). The binding perturbation imposed by the changes at Phe-31 increases K_D for all folate analogues with a larger increase for MTX. The mutation has little effect on the K_D for NADPH, implying that the perturbation occurs only at the H_2F binding site, as expected, since Phe-31 resides at the H_2F site.

The dissociation constants for DAM could not be determined by the above-mentioned enzyme fluorescence

(40) Birdsall, B.; Burgen, A. S. V.; Roberts, G. C. K. *Biochemistry* **1980**, *19*, 3723–3732.

(41) Stone, S. R.; Morrison, J. F. *Biochim. Biophys. Acta* **1986**, *869*, 275–285.

(42) Stone, S. R.; Morrison, J. F. *Biochem. Biophys. Acta* **1983**, *745*, 247–258.

Table II. Thermodynamic Dissociation Constants (K_D) for Binary Complexes (DHFR·L) and Inhibition Constants (K_I) for the DHFR·NADPH·DAM Ternary Complexes[a]

ligand	DHFR	K_D, μM pH 6.0	pH 7.0	pH 8.0	pH 8.5	pH 9.5	K_I, μM pH 5.5
H_2F	Phe-31		0.21 ± 0.03		0.24 ± 0.03		
	Tyr-31		2.6 ± 0.3		2.9 ± 0.2		
	Val-31		6.6 ± 0.5		6.2 ± 0.8		
NADPH	Phe-31		0.38 ± 0.04		0.49 ± 0.06		
	Tyr-31		0.34 ± 0.03		0.40 ± 0.02		
	Val-31		0.22 ± 0.02		0.30 ± 0.03		
H_4F	Phe-31		0.06 ± 0.02				
	Tyr-31		0.3 ± 0.1				
	Val-31		0.3 ± 0.1				
Folate	Phe-31		0.81 ± 0.07				
	Tyr-31		4.4 ± 0.1				
	Val-31		4.8 ± 0.4				
MTX	Phe-31	0.000 023 ± 0.000 076		0.000 96 ± 0.000 48		0.031 ± 0.002	
	Tyr-31	0.0023 ± 0.0007		0.14 ± 0.01		1.7 ± 0.01	
	Val-31	0.0032 ± 0.0017		0.084 ± 0.012		1.1 ± 0.1	
DAM	Phe-31	1.6 ± 0.3[b]					0.044[c]
	Tyr-31	3.9 ± 0.8[b]					0.057
	Val-31	-[d]					9.1

[a] The thermodynamic dissociation constants (K_D) were measured by following the decrease in enzyme fluorescence at 340 nm upon formation of the binary complexes at 25 °C in MTEN buffer. The inhibition constants were determined from Dixon plots based on steady-state experiments carried out at 25 °C and pH 5.5 in MTEN buffer. [b] The dissociation constants of DAM from DHFR·DAM were measured by monitoring the decrease of DAM fluorescence at 450 nm upon addition of DHFR which occurs on the protonation of DAM at the active site. [c] Calculated on the basis of the pH-independent value of 0.013 μM and eq 10 of ref 42. [d] Unable to be measured.

Table III. MTX Binding to DHFR (*E. coli*) at 25 °C and pH 6.0

constants	DHFR Phe-31	Tyr-31	Val-31
k_{on} (M^{-1} s^{-1})	3.6×10^7	1.1×10^7	1.5×10^5
k_{off} (s^{-1})	12	26	26
k_f (s^{-1})[a]	0.17×10^3	1.08×10^3	21×10^3
k_r (s^{-1})	0.0051	0.20	0.048
K_i (μM)[b]	0.33	2.4	170
K_{iso}[c]	33×10^3	5.4×10^3	440×10^3
K_D (nM)[d]	0.023	2.3	3.2
K_{eq}[e]	0.72	0.24	0.14

[a] Calculated by employing eq 3. [b] Calculated from k_{off}/k_{on}. [c] Calculated from k_f/k_r. [d] Overall thermodynamic dissociation constants. [e] Taken from ref 17.

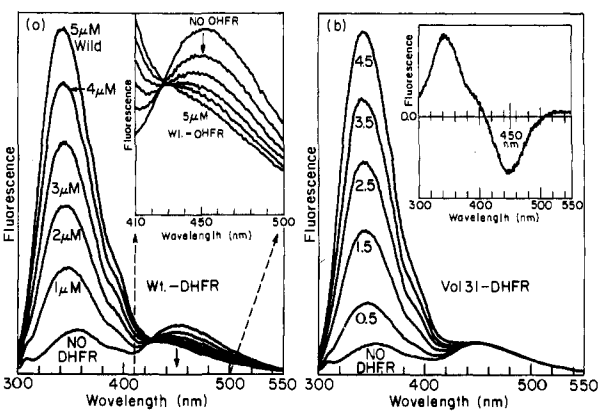

Figure 5. Change of DAM fluorescence upon addition of DHFR at 25 °C and pH 6.0 in MTEN buffer. (a) To a solution of 2.0 μM DAM was added wild-type DHFR to yield the final enzyme concentration of 1, 2, 3, 4, and 5 μM. In the insert, the wavelength 410–500 region is expanded in order to show the fluorescence decrease at 450 nm upon addition of the wild-type DHFR. (b) To a solution of 2.0 μM DAM was added Val31-DHFR to the final enzyme concentration of 0.5, 1.5, 2.5, 3.5, and 4.5 μM. In the insert is shown a difference fluorescence spectrum of DAM (pH 5.0–10.0) demonstrating the fluorescence decrease at 450 nm upon protonation of DAM.

quenching technique since DAM itself has significant fluorescence at 340 nm, the wavelength at which the enzyme fluorescence is normally monitored. The fluorescence emission spectrum for DAM, which has two emission maxima at 355 and 450 nm, is shown in Figure 5 labeled as "No DHFR". An examination of an emission spectrum can generally provide information on the environment surrounding a fluorophore. When the environment of a fluorophore becomes less polar due to, for example, a relocation of the fluorophore from an aqueous phase to an enzyme active site, the relative quantum yield generally increases, accompanied by a shift of the emission maximum to a shorter wavelength. The emission maximum of DAM at 450 nm, however, decreases upon addition of wild-type DHFR to the solution containing DAM (Figure 5a). In order to show this decrease more clearly, the region between 410 and 500 nm is expanded in the insert of Figure 5a). The increase at 340 nm is obviously due to the addition of more fluorescent enzyme. A similar phenomenon was observed upon addition of the Tyr-31 mutant enzyme to a DAM solution (data not shown). In contrast, as shown in Figure 5b, the addition of Val-31 did not affect the fluorescence amplitude at 450 nm. When a heat-denatured wild-type DHFR (heated at 70 °C for 10 h) was employed for the titration, the series of fluorescence emission spectra were identical with that for Val31-DHFR; there was no change in fluorescence at 450 nm, suggesting that in the two experiments no DAM was bound.

The decrease in fluorescence at 450 nm, thus, has been confirmed to originate from the binding of DAM to the DHFR active site. The quantum yield has diminished upon binding of DAM to the less polar cleft because DAM becomes protonated by a proton transfer most likely from Asp-27. A difference fluorescence spectrum, obtained by subtracting the DAM spectrum at pH 10.0 from that at pH 5.0, is shown in the insert of Figure 5b, which clearly demonstrates the decrease at 450 nm accompanying an increase at 340 nm upon protonation of DAM. This is in agreement with Stone and Morrison's finding,[42] based on ultraviolet difference spectroscopy, that DAM, when bound to the enzyme, exists in its protonated form. A plot of the fluorescence at 450 nm versus the concentration of DHFR yielded a calculated dissociation constant (eq 8) of 1.38×10^{-6} M for the wild-type DHFR. Since the fluorescent

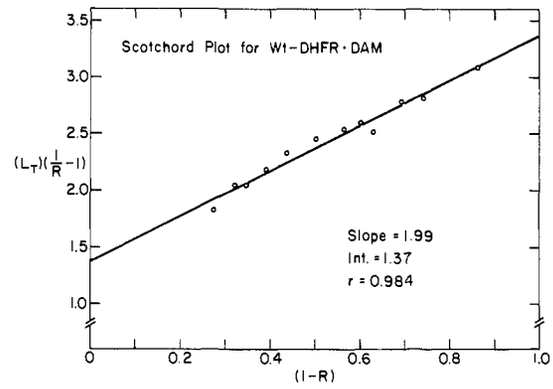

Figure 6. Scatchard plot for the binding of wild-type DHFR and DAM. The plot was produced by employing eq 15.

Scheme IV

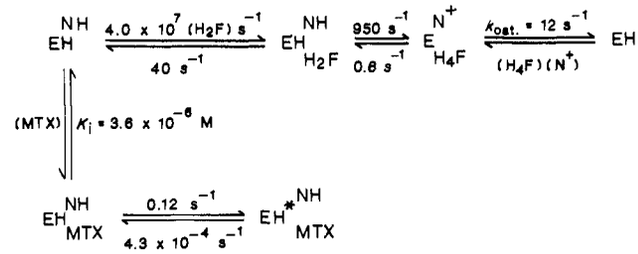

species in this case is DAM, E_T, F_E, and L_T in eq (8) were treated as the total concentration of DAM (2 μM), the fluorescence of DAM, and the total concentration of DHFR, respectively. A similar treatment for Tyr-31 provided the best-fit dissociation constant of 3.9×10^{-6} M.

The Scatchard plot, shown in Figure 6, for wild-type DHFR provides further evidence that the decrease in fluorescence at 450 nm is caused by the binding of DAM. From the linear plot of $(L_T)(1/R - 1)$ versus $(1 - R)$, a value of K_D equal to 1.37 μM (intercept) and the total binding site concentration (nE_T) of 1.99 μM (slope) can be calculated by employing eq 16. In this case R denotes the ratio of the DHFR·DAM complex to the total concentration of DAM, $[DHFR{\cdot}DAM]/[DAM]_T$, which can be determined by monitoring fluorescence at 450 nm. The difference between the initial fluorescence of DAM itself (F_E) and the end-point fluorescence (F_{EL}) corresponds to $[DAM]_T$, and the difference between F_E and the fluorescence (F) upon partial addition of DHFR corresponds to the amount of complex formed (DHFR·DAM). The end point employed (F_{EL}) was the value (49%) obtained by the above-mentioned computer fitting of the fluorescence titration data. Since E_T denotes the total DAM concentration of 2.0 μM, the division of the slope (nE_T = 1.99 μM) by E_T (2.0 μM) provides the number of ligands bound as one. Although it is known[43] that H_2F, at higher concentrations, causes substrate inhibition by combining at the NADPH binding site on the enzyme to form a $H_2F{\cdot}DHFR{\cdot}H_2F$ ternary complex, an n of unity for DAM binding clearly demonstrates that DAM binds only to the H_2F binding site.

Discussion

Kinetic Description of MTX Binding. Methotrexate (MTX) has been characterized as a slow, tight-binding inhibitor of avian as well as bacterial dihydrofolate reductases (DHFR).[37,38,41] An abbreviated, combined kinetic sequence for catalysis by wild-type DHFR (*E. coli*) at low pH[39] and for tight-binding inhibition[41] by MTX is illustrated in Scheme IV. The rate constants associated with the tight-binding inhibition have been obtained by analyzing the steady-state progress curve[41,44] for the inhibition in the presence of saturating NADPH. For dissecting the mode of inhibition with respect to the apoenzyme (EH), however, the progress curve technique is not applicable. Thus, we turned to stopped-flow kinetics combined with thermodynamic fluorescence titration as our methods of choice.[35-38,40]

Scheme V

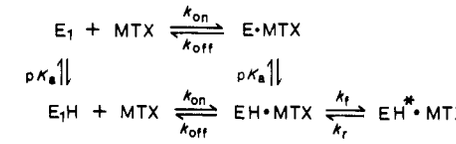

Analysis of MTX binding to the apoenzyme (EH) has a potential complication, unlike the case of holoenzyme (E^{NH}), owing to the inhibitor's ability to bind to both forms of the enzyme.[36] Recall in Scheme I that substrates such as H_2F and NADPH are capable of binding to only one form (E_1) of the apoenzyme; moreover, the resulting holoenzyme ($E_1{\cdot}L_1$) has only one conformer to which H_2F analogues bind.[34-36] This potential complication may be avoided by measuring the initial binding rate of MTX to E_1 (fast phase) that is characterized by a single MTX-dependent exponential as in Figure 2a. The measured association and dissociation rate constants for formation of the initial complex are listed in Table I. The association rate constants for MTX are pH-independent (see also footnotes *d* and *f* of Table I), as they are for substrate binding.[39] However, contrary to the pH independence of the substrate's overall K_D, which stems from the fact that substrates have one binding step with pH-independent on/off rate constants, the overall K_D's for MTX are pH-dependent (Table II). These K_D values are significantly smaller than the dissociation constants for the initial complexes ($K_i = k_{off}/k_{on}$). These results demand that a proton is required for the tight-binding isomerization ($K_{iso} = k_f/k_r$) of the initial complex as described in Scheme V. More precisely, the rate constants for formation of the initial binary complexes are independent of the ionization state of the Asp-27 (pK_a of Wt.-DHFR is 6.5,[39] this pK_a is absent in the Asn-27 mutant[26]) although isomerization to form the tight complex (EH*·MTX) only occurs within the protonated form. Owing to this isomerization step, the dissociation rate constants (k_r) of MTX from the EH*·MTX complexes, measured by competition experiments, are much smaller than the off rate (k_{off}) from the initial complex, determined as the intercept of a linear plot of k_{obsd} vs [MTX]. For example, as shown in Figure 3b for Val31-DHFR, the intercept (k_{off}) is 26 s^{-1} whereas k_r has a much smaller value of 0.048 s^{-1} (see also Table I).

In contrast to MTX, the inhibitor 2,4-diamino-6,7-dimethylpteridine (DAM), a MTX analogue lacking the (*p*-aminobenzoyl)glutamate side chain, binds to protonated DHFR in a single step with a rate constant slightly smaller than that of MTX but without further isomerization to a tighter species (Table I). In the case of Tyr31-DHFR, the k_{off} (24.9 s^{-1}) measured from the time-dependent fluorescent quenching matches the rate of dissociation (24.6 s^{-1}) determined by a competition experiment. Similar results were obtained for wild-type DHFR; however, in the case of Val31-DHFR, K_i appeared to be too large to be measured by these techniques. DAM appears to bind less

(43) Stone, S. R.; Morrison, J. F. *Biochemistry* **1982**, *21*, 3757–3765.

(44) Williams, J. W.; Morrison, J. F.; Duggleby, R. G. *Biochemistry* **1979**, *18*, 2567–2573.

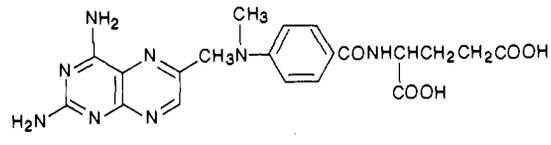

MTX (methotrexate)

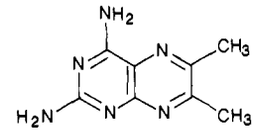

DAM (2,4-diamino-6,7-dimethylpteridine)

tightly to unprotonated DHFR as evidenced by the increase in K_D at high pH.[42]

Effect of Active Site Mutagenesis. In studying mutant proteins, an important initial question to address is that of their structural integrity. Recent crystallographic studies indicate that point mutations are in general accommodated by very minor readjustments of the tertiary protein structure with water molecules occupying the space created by a smaller amino acid α-side chain.[26,45,46] We have examined thermodynamic dissociation constants as well as kinetic on/off rate constants to assess the potential effect of the single amino acid change upon structure. The mutation of Phe-31 which resides at the base of the H_2F binding cleft (Figure 1) had little effect on the binding of NADPH (Table II). The earlier mutation of His-45 (to Gln), which removed a potential interaction between the imidazole moiety and the pyrophosphate backbone of NADPH, was shown to alter both the association and dissociation rate constants for the cofactor so that the dissociation constant was increased 6–40-fold.[16] However, this mutation (His-45 → Gln) neither affected the dissociation constants (K_D) for H_2F, H_4F, folate, and MTX nor changed the association rate constant for MTX (data not shown). These results clearly reveal that a mutation at the H_2F or the NADPH binding site does not translate its effect onto the other binding pocket: the perturbation is very local.

Kinetic analysis of MTX binding to our mutants at the invariant Phe-31 residue at pH 6.0 (25 °C) has been determined according to Scheme V but with a correction, as noted earlier, for the level of E_1H (Scheme III). The overall thermodynamic dissociation constant (K_D) is given by

$$K_D = K_i(1 + 1/K_{eq})/(1 + K_{iso}) \quad (2)$$

where $K_i = k_{off}/k_{on}$, $K_{iso} = k_f/k_r$, and K_{eq} is defined in Scheme III. The forward isomerization constant (k_f) can be calculated from the rearranged form of eq 2.

$$k_f = k_r[[K_i(1 + 1/K_{eq})/K_D] - 1] \quad (3)$$

We make the assumption that the ground states of the wild-type and mutants are equal in stability. On the basis of this assumption, an energy diagram for the binding of MTX has been constructed in Figure 7, and the constants utilized for construction of the diagram are summarized in Table III.

Although the association rate constants (k_{on}) for substrates and inhibitors lie in the small range of just above 10^7 M^{-1} s^{-1} at 25 °C for the wild-type DHFR,[36,39] the most marked difference occurs with the Val-31 mutant in which k_{on} for MTX is reduced by a factor of 240. This slower on rate appears to be general for the Val-31 since k_{on} for

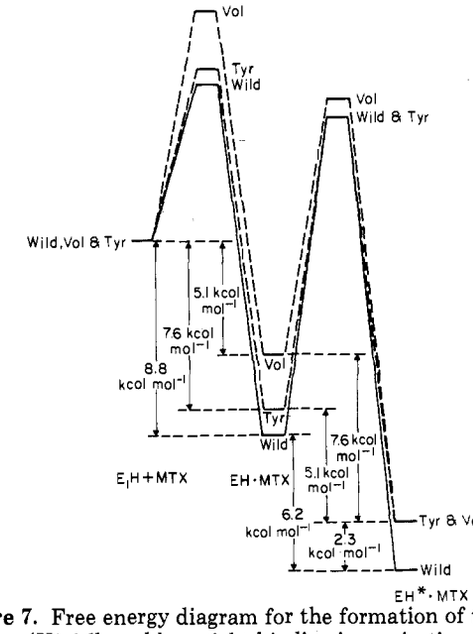

Figure 7. Free energy diagram for the formation of the initial complex (K_i) followed by a tight-binding isomerization step (K_{iso}) comparing wild-type DHFR to two mutant enzymes.

TMP is also in the order of 10^5 M^{-1} s^{-1} (data not shown). Although the rates of inhibitor binding (k_{on}) generally seem to be unaffected by the presence of a bound coenzyme for *E. coli* wild-type DHFR as well as the Gln-45 mutant, in agreement with the finding of Dunn and King for *L. casei* DHFR,[34] k_{on} for the Val-31 enzyme in the presence of NADPH increases almost 2 orders of magnitude, approximating the value for wild-type DHFR as shown in Figure 3. Tight-binding inhibition is characterized by isomerization of an initial enzyme–inhibitor (EH·MTX) complex that leads to the formation of a more stable complex. In order for this isomerization to occur, the *p*-aminobenzoyl moiety plays a key role since there is no evidence that DAM, which lacks the side chain, undergoes isomerization (Tables I and II). It is conceivable but speculative that this process involves an ca. 180° rotation around the C-6–C-9–N-10 bond axis with the pteridine ring of MTX initially in an orientation similar to that of the pterin ring of bound H_2F.

For the binding of the pteridine moiety, aromatic–aromatic interactions appear to be very important. Recall that Phe-31 is located in a hydrophobic pocket and interacts with the pteridine ring through van der Waals contacts in the EH·MTX complex so that the edge of the phenyl ring is oriented toward both faces of the pteridine ring and *p*-aminobenzoyl group (Figure 1).[4] The edge-to-face aromatic–aromatic interaction is very common in proteins and plays an important role in tertiary structure stabilization.[47] Thus, upon mutation to Tyr-31 the binding interactions with DAM are conserved (Table II). In contrast, the Phe-31 → Val mutation increases the K_I over 200-fold (corresponding to a decrease in binding energy of 3.1 kcal/mol). The ratio K_D/K_I for DAM, which reflects the synergism exerted by NADPH on the binding of DAM, is 36 and 68 for Phe-31 and Tyr-31, respectively, in agreement with the reported value of 60 at 30 °C and pH 6.4 for Phe-31.[41] If we assume a synergism of similar magnitude for Val-31, the expected K_D would be over 300 μM, too large to measure with the techniques employed in this study (e.g., Figure 5b).

(45) Straus, D.; Kawashima, R. E.; Knowles, J. R.; Gilbert, W. *Proc. Natl. Acad. Sci. U.S.A.* **1985**, *82*, 2272–2276.
(46) Chothia, C.; Lesk, A. M. *J. Mol. Biol.* **1985**, *182*, 151–158.
(47) Burley, S. K.; Petsko, G. A. *Science (Washington, D.C.)* **1985**, *229*, 23–28.

With MTX, the influence of Val-31 is to decrease the stability of the initial and final binary complexes by 3.7 and 2.3 kcal/mol, respectively. The replacement of Phe-31 by Val sacrifices 2.9 kcal/mol of the binding energy reflecting the loss of hydrophobic interactions. The less favorable (1–2 kcal/mol) Tyr-31 interactions in the formation of either binary complex may have a steric origin owing to the extra volume exerted by the hydroxyl group which may have a sterically unfavorable interaction with the *p*-aminobenzoyl moiety.

The changes in the values of K_D for H_2F, H_4F, and folate parallel those for MTX, with the weaker binding affinity for H_2F compared to MTX (210 nM vs 0.023 nM) (5.4 kcal/mol) reflecting the absence of the salt bridge, possible hydrogen bonding from the amide backbone to the 4-NH_2 of MTX, and less favorable interaction with Phe-31. The binding perturbation imposed by the changes at Phe-31 increases K_D for all three ligands but to a lesser degree than for MTX. Thus, interactions between Phe-31 and ligand are more important for inhibitor (MTX) binding than for substrate (H_2F, H_4F, folate) binding which may be due to the difference in orientation between bound substrate and inhibitor.

With this information it is not difficult to explain the alteration in the human DHFR gene during the development of a MTX-resistant human cell line.[48] After stepwise selection in increasing concentrations of MTX, a resistant subline has developed that can grow in the presence of 100 μM MTX. The only alteration found is a T to C substitution at codon 31 that causes a Phe-31 to Ser-31 mutation. Although owing to a differing numbering this mutation is not analogous to the ones described here (this site is equivalent to the Leu-28 in *E. coli*, which also interacts with MTX), nevertheless the reduced MTX binding reflects an anticipated reduced hydrophobic interaction of greater importance for MTX than H_2F.

In summary, the combination of the techniques of site-directed mutagenesis and transient kinetics has been used to probe the role of individual amino acids at the active site of dihydrofolate reductase in drug binding. DAM is unambiguously shown to be a classical inhibitor for the DHFR apoenzyme, and it clearly binds in its protonated form to the enzyme, possessing a strong interaction with the Phe-31 residue. A comparison of MTX binding to DHFR mutants at residues Asp-27 and Phe-31 has suggested that hydrophobic interactions between MTX and DHFR are at least as important as the formation of a DHFR·MTX salt bridge as a determinant of the tight binding of MTX.

Experimental Section

Materials. 7,8-Dihydrofolate (H_2F) was prepared from folic acid by the method of Blakley,[49] and (6*S*)-tetrahydrofolate (H_4F) was prepared from H_2F by using dihydrofolate reductase[50] and purified on DE-52 resin eluting with a triethylammonium bicarbonate linear gradient.[51] Reduced nicotinamide adenine dinucleotide phosphate (NADPH), nicotinamide adenine dinucleotide phosphate ($NADP^+$), trimethoprim (TMP), methotrexate (MTX), and folic acid were purchased from Sigma. 2,4-Diamino-6,7-dimethylpteridine (DAM) was purchased from ICN Pharmaceuticals. The concentrations of the ligands were determined spectrophotometrically by using the molar extinction coefficients given below: H_2F, 28 000 M^{-1} cm^{-1} (282 nm, pH 7.5);[52] H_4F, 28 000 M^{-1} cm^{-1} (297 nm, pH 7.5);[53] folic acid, 28 000 M^{-1} cm^{-1} (281 nm, pH 7.0); TMP, 5800 M^{-1} cm^{-1} (271 nm, in 0.1 M acetic acid); MTX, 23 000 or 22 100 M^{-1} cm^{-1} (257 or 302 nm, respectively, in 0.1 M KOH);[54] DAM, 6900 or 7200 M^{-1} cm^{-1} (346 nm at pH 6.0 or 364 nm at pH 8.0, respectively);[55] NADPH, 6200 M^{-1} cm^{-1} (339 nm, pH 8.5);[56] $NADP^+$, 18 000 M^{-1} cm^{-1} (259 nm, pH 8.5). The concentration of H_4F was also determined enzymatically by using a molar absorbancy change for the 10-formyl synthetase reaction of 12 000 M^{-1} cm^{-1} at 312 nm.[57] The concentrations of H_2F and NADPH were also determined enzymatically by using a molar absorbancy change for the dihydrofolate reductase reaction of 11 800 M^{-1} cm^{-1} at 340 nm.[43]

The Tyr-31 and Val-31 mutants were constructed, as previously described,[29] by primer extension of oligonucleotides[20] using as the template partially single stranded plasmid DNA, pTY1, in which a 1-kilobase fragment containing the DHFR gene (*fol*)[58] was inserted into the *Bam* HI site of a 4.4-kilobase pBR322 derivative DNA lacking the *Eco* RI site. Wild-type as well as mutant DHFR was purified from *E. coli* strain HB101 containing the appropriate *fol* plasmid using a methotrexate affinity resin.[29,59] The concentration of purified DHFR was determined spectrophotometrically at 280 nm by using a molar extinction coefficient of 31 100 M^{-1} cm^{-1} or by methotrexate titration.[44]

Methods. All measurements were performed at 25 °C in a buffer containing 34 mM 2-morpholinoethanesulfonic acid (MES), 25 mM tris(hydroxymethyl)aminomethane (Tris), 25 mM ethanolamine, and 100 mM NaCl (MTEN buffer).[10,60]

Steady-State Kinetics. Initial velcities (v) for the dihydrofolate reductase reactions were determined by measuring the rate of the enzyme-dependent decrease of H_2F and NADPH at 340 nm with a molar absorbancy change[43] of 11 800 M^{-1} cm^{-1} employing a Cary 219 spectrophotometer. The concentration of NADPH was maintained constant at a saturating level of 60 μM. The inhibition constant of DAM, K_I (the dissociation constant of DAM from the DHFR·NADPH·DAM ternary complex), was obtained by plotting $1/v$ vs the inhibitor (DAM) concentration (Dixon plot).[61]

Transient Kinetics. Pre-steady-state kinetic data were obtained by using a stopped-flow apparatus operating in the fluorescence mode, which was built by Professor K. A. Johnson[62] and possesses a 1.6-ms dead time, a 2-mm path length, and a thermostated sample cell. Interference filters (Corion Corp.) were used on both the light input (excitation) and output (emission). In most cases the formation of the complex was followed by using a 290-nm interference filter on the excitation input and then monitoring the quenching of the intrinsic enzyme fluorescence with an output filter at the emission wavelength of 340 nm.[34,63] For the measurement of the NADPH dissociation rate constant, the enhancement of coenzyme fluorescence by energy transfer was followed by using a 290-nm interference filter on the input and a 450-nm filter on the output. For slow reactions such as

(48) Schweitzer, B. I.; Srimatkandada, S.; Dube, S. K.; Bertino, J. R. In *Chemistry and Biology of Pteridines 1986*; Cooper, B. A., Whitehead, V. M., Eds.; Walter de Gruyer: Berlin, 1986; p 793–797.
(49) Blakley, R. L. *Nature (London)* **1960**, *188*, 231–232.
(50) Mathews, C. K.; Huennekens, F. M. *J. Biol. Chem.* **1960**, *235*, 3304–3308.
(51) Curthoys, H. P.; Scott, J. M.; Rabinowitz, J. C. *J. Biol. Chem.* **1972**, *247*, 1959–1964.
(52) Dawson, R. M. C.; Elliott, D. C.; Elliott, W. H.; Jones, K. M. *Data for Biochem. Res.*; Oxford University: Oxford, 1969.
(53) Kallen, R. G.; Jencks, W. P. *J. Biol. Chem.* **1966**, *241*, 5845–5850.
(54) Seeger, D. R.; Cosulich, D. B.; Smith, J. M.; Hultquist, M. E. *J. Am. Chem. Soc.* **1949**, *71*, 1753–1758.
(55) Brown, D. J.; Jacobsen, N. W. *J. Chem. Soc.* **1961**, 4413–4420.
(56) *P.-L. Biochemicals*; Circular OR-18; P.-L. Biochemicals: Milwaukee, WI, 1961.
(57) Smith, G. K.; Benkovic, P. A.; Benkovic, S. J. *Biochemistry* **1981**, *20*, 4034–4036.
(58) Smith, D. R.; Calvo, J. M. *Nucleic Acids Res.* **1980**, *8*, 2255–2274.
(59) Kaufman, B. T. *Methods Enzymol.* **1974**, *34*, 272–281.
(60) Ellis, K. J.; Morrison, J. F. *Methods Enzymol.* **1982**, *87*, 405–426.
(61) Segel, I. H. *Enzyme Kinetics, Behavior and Analysis of Rapid Equilibrium and Steady-State Enzyme Systems*; Wiley: New York, 1975; p 109.
(62) Johnson, K. A. *Methods Enzymol.* **1986**, *134*, 677–705.
(63) Lakowicz, J. R. *Principles of Fluorescence Spectroscopy*; Plenum: New York, 1983.

MTX dissociation, a neutral density filter (0.2–2.0 OD) was placed on the input to decrease the light intensity and thus decrease photobleaching of the sample. For measurements of fluorescence changes, the final DHFR concentration was 0.14–3.0 μM and ligand concentrations were adjusted so that the observed rate constants (k_{obsd}) did not exceed 200 s^{-1}. In most experiments the average of at least four runs was used for data analysis.

Data were collected by a computer over a given time interval following a trigger impulse, until a few milliseconds before stop, and stored on a floppy disk.[62] The data then were graphically displayed and analyzed by using either a single-exponential model (for most ligands)

$$F(t) = \text{AMP} \exp(-k_{obsd}t) + \text{base line} \quad (4)$$

or a double-exponential model (for MTX binding)

$$F(t) = \text{AMP}_{fast} \exp(-k_{fast}t) + \text{AMP}_{slow} \exp(-k_{slow}t) + \text{base line} \quad (5)$$

where $F(t)$ is the observed fluorescence at time t, AMP, AMP_{fast}, and AMP_{slow} are the amplitude terms for the fluorescence change, and k_{obsd}, k_{fast}, and k_{slow} are the rate constants.

Fluorescence Titrations. Thermodynamic dissociation constants (K_D) were determined by fluorescence titration employing a SLM 8000 spectrofluorimeter. The formation of the enzyme–ligand complex was followed by measuring the quenching of the tryptophan fluorescence of the enzyme upon addition of microliter volumes of a concentrated ligand stock solution. Unless otherwise stated, an excitation wavelength of 290 nm was used together with an emission wavelength of 340 nm.[40-42,63,64] For the titration with H_4F, an emission wavelength of 328 nm was employed with the excitation and emission slits set at 2 nm in order to minimize the fluorescence due to the H_4F sample. In order to measure a dissociation constant with reasonable precision, the enzyme concentration must be less than $\sim^1/_2K_D$; this condition could not be met for the titration with MTX at low pH. For this MTX titration, the enzyme concentration employed was 5 nM ($>K_D$) with the excitation and emission slits set at 8 nm and 16 nm, respectively, to maximize the signal. A solution of tryptophan with a fluorescence similar to that of the enzyme solution was used to determine the correction factor for inner filter effects. The decrease in intensity due to an absorbing ligand at the excitation or the emission wavelength was then added to the fluorescence of the protein to compensate for the inner filter effect.

The dissociation constant of the binary complex between the enzyme and DAM was determined by measuring the decrease of the DAM fluorescence at 450 nm, at which there is no interference due to the fluorescence of the enzyme, upon addition of microliter volumes of a concentrated stock solution of DHFR. During the titration of DAM with DHFR, an excitation wavelength of 280 nm and an emission wavelength of 450 nm were used with the excitation and emission slits set at 4 nm and 8 nm, respectively.

Since the dissociation constant (K_D) for the enzyme–ligand complex is given by

$$K_D = (E_T - \text{EL})(L_T - \text{EL})/(\text{EL}) \quad (6)$$

where (L_T) represents the total ligand concentration, the expression for (EL), the concentration of the enzyme–ligand complex, can be obtained as

$$(\text{EL}) = \{(E_T + L_T + K_D) - [(E_T + L_T + K_D)^2 - 4(E_T)(L_T)]^{1/2}\}/2 \quad (7)$$

Since (E) = (E_T – EL), the expression for the observed fluorescence (F) can be written in terms of five constants (E_T, L_T, K_D, F_E, and F_{EL}):

$$F = F_E - C(F_E - F_{EL})/(2E_T) \quad (8)$$

where $A = (E_T + L_T + K_D)$, $B = [A^2 - 4(E_T)(L_T)]^{1/2}$, and $C = A - B = 2(\text{EL})$. Measurements of the observed enzyme fluorescence (F) at various concentrations of a ligand (L_T), typically 15–20 points, enable one to fit the data by utilizing a nonlinear least squares fitting program, NLIN (Marquardt Method).[65] The remaining four parameters (E_T, K_D, F_E, F_{EL}) are treated as unknowns, employing the following four derivatives with respect to each unknown.

$$\partial F/\partial E_T = (F_{EL} - F_E)[1 - (E_T + K_D - L_T)/B - C/E_T]/(2E_T) \quad (9)$$

$$\partial F/\partial K_D = (F_{EL} - F_E)(1 - A/B)/(2E_T) \quad (10)$$

$$\partial F/\partial F_E = 1 - C/(2E_T) \quad (11)$$

$$\partial F/\partial F_{EL} = C/(2E_T) \quad (12)$$

In order to check the internal consistency, the number of unknown parameters is reduced to three, by keeping either F_E or E_T at constant values of 100% or the initial enzyme concentration, respectively, and eventually to two unknowns (K_D and F_{EL}) by employing the known best values for E_T and F_E.

Scatchard Plot. If there are n identical ligand binding sites on the enzyme, eq 6 may be modified to

$$K_D = (E_T - \text{EL})(L_T - n\text{EL})/(\text{EL}) \quad (13)$$

where (E_T – EL) and (L_T – nEL) represent the concentrations of free enzyme (E) and free ligand (L), respectively. Equation 13 can be expanded to eq 14 and rearranged into eq 15 or 16, where

$$K_D = (E_T)(L_T)/(\text{EL}) - (L_T) - nE_T + n\text{EL} \quad (14)$$

$$K_D = (L_T)(E_T/\text{EL} - 1) - nE_T(1 - \text{EL}/E_T) \quad (15)$$

$$(L_T)(1/R - 1) = K_D + nE_T(1 - R) \quad (16)$$

R denotes the ratio of the enzyme–ligand complex to the total enzyme, (EL)/(E_T), which can be determined from the above-mentioned fluorescence titrations since (EL) = (F_E – F) and (E_T) = (F_E – F_{EL}). Plotting (L_T)(1/R – 1) vs (1 – R) (eq 16) provides the dissociation constant (K_D), as the intercept, and the total concentration of ligand binding sites (nE_T) as the slope. The number of ligand binding sites (n) also can be obtained, by dividing the slope by the total enzyme concentration (E_T).

Acknowledgment. We appreciate the collaboration of J.-T. Chen during the preparation and the analysis on the catalytic events of the mutant enzymes, the very stimulating comments of C. A. Fierke and K. A. Johnson, the many helpful suggestions of D. J. Allen and R. J. Miller, and preparation of H_4F by L. F. Courtney. We also thank Kaye Yarnell for her constant help with the manuscript.

Registry No. MTX, 59-05-2; DAM, 1425-63-4; DHFR, 9002-03-3; L-Phe, 63-91-2.

(64) Birdsall, B.; Burgen, A. S. V.; Rodriques de Miranda, J.; Roberts, G. C. K. *Biochemistry* **1978**, *17*, 2102–2109.

(65) *SAS User's Guide: Statistics, Version* 5 Edition, The NLIN Procedure; SAS Institute: Cary, NC, 1985; Chapter 25.